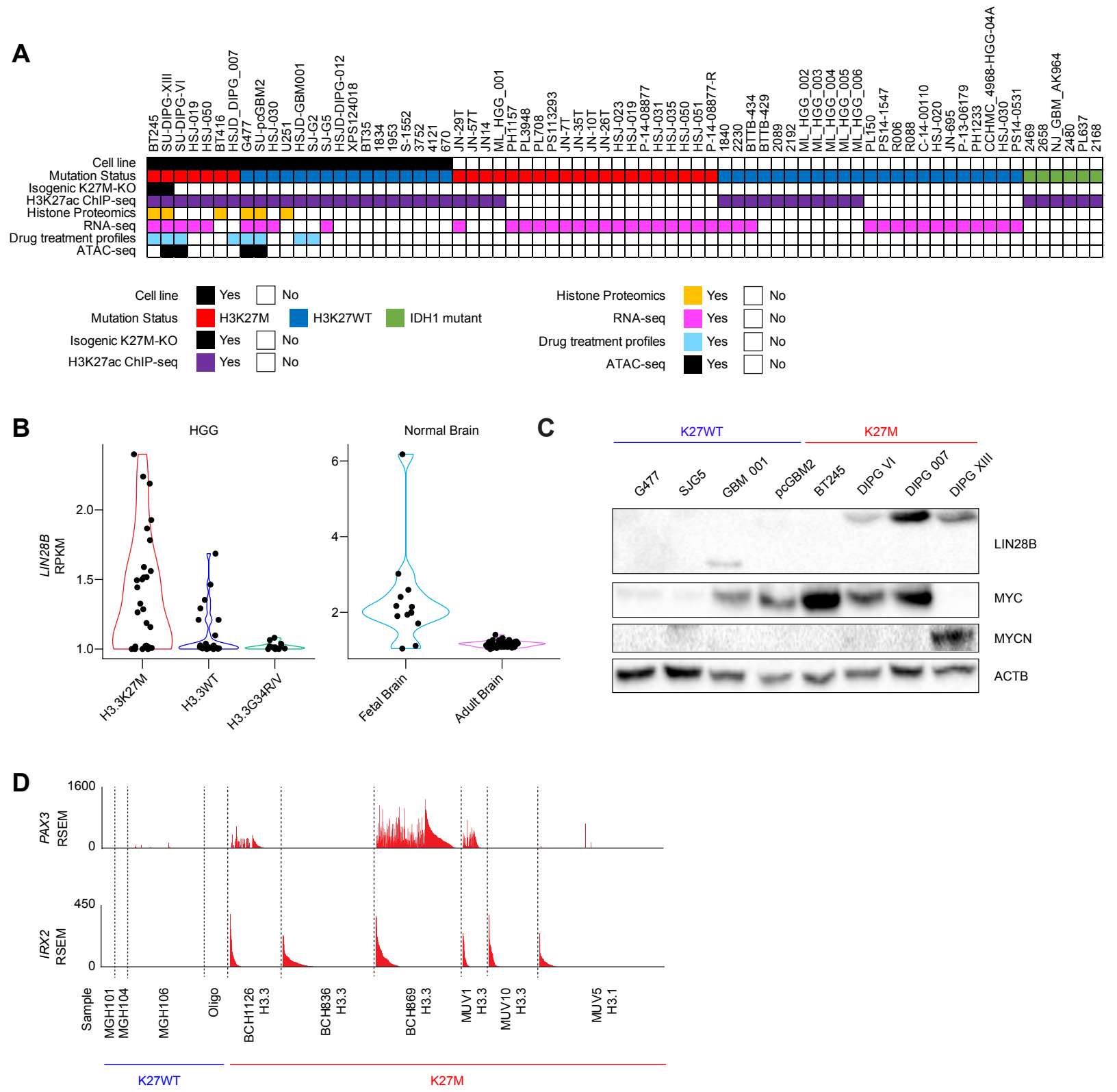
A
BT245
SU-DIPG-XIII
SU-DIPG-VI
HSJ-019
HSJ-050
BT416
HSJD_DIPG_007
G477
SU-pcGBM2
HSJ-030
U251
HSJD-GBM001
SJ-G2
SJ-G5
HSJD-DIPG-012
XPS124018
BT35
1834
1953
S-1552
3752
4121
670
JN-29T
JN-57T
JN14
ML_HGG_001
PH1157
PL3948
PL708
PS113293
JN-7T
JN-35T
JN-10T
JN-26T
HSJ-023
HSJ-019
P-14-08877
HSJ-031
HSJ-035
HSJ-050
HSJ-051
P-14-08877-R
1840
2230
BTTB-434
BTTB-429
2089
2192
ML_HGG_002
ML_HGG_003
ML_HGG_004
ML_HGG_005
ML_HGG_006
PL150
PS14-1547
R006
R088
C-14-00110
HSJ-020
JN-695
P-13-06179
PH1233
CCHMC_4968-HGG-04A
HSJ-030
PS14-0531
2469
2658
NJ_GBM_AK964
2480
PL637
2168
Cell line
Mutation Status
Isogenic K27M-KO
H3K27ac ChIP-seq
Histone Proteomics
RNA-seq
Drug treatment profiles
ATAC-seq
Cell line Yes No
Mutation Status H3K27M H3K27WT IDH1 mutant
Isogenic K27M-KO Yes No
H3K27ac ChIP-seq Yes No
Histone Proteomics Yes No
RNA-seq Yes No
Drug treatment profiles Yes No
ATAC-seq Yes No
B
HGG
Normal Brain
LIN28B RPKM
2.0
1.5
1.0
6
4
2
H3.3K27M
H3.3WT
H3.3G34R/V
Fetal Brain
Adult Brain
C
K27WT
K27M
G477
SJG5
GBM 001
pcGBM2
BT245
DIPG VI
DIPG 007
DIPG XIII
LIN28B
MYC
MYCN
ACTB
D
PAX3 RSEM
1600
0
IRX2 RSEM
450
0
Sample
MGH101
MGH104
MGH106
Oligo
BCH1126 H3.3
BCH836 H3.3
BCH869 H3.3
MUV1 H3.3
MUV10 H3.3
MUV5 H3.1
K27WT
K27M

Figure S1. Related to Figure 1.
(A) List of tumors, xenograft models, and cell lines used in this study and the datasets generated.
(B) Expression (RPKM) of *LIN28B* across a panel of high-grade gliomas (H3.3K27M, H3.3WT and H3.3G34R/V) and normal brain tissues (fetal and adult brain).
(C) Western blot of LIN28B, MYC and MYCN proteins across a panel of H3K27WT and H3.3K27M pHGG cell lines.
(D) Single cell profiling of *IRX2* and *PAX3* across GBM and HGG-H3K27M samples derived from Filbin et al. (Filbin et al., 2018).

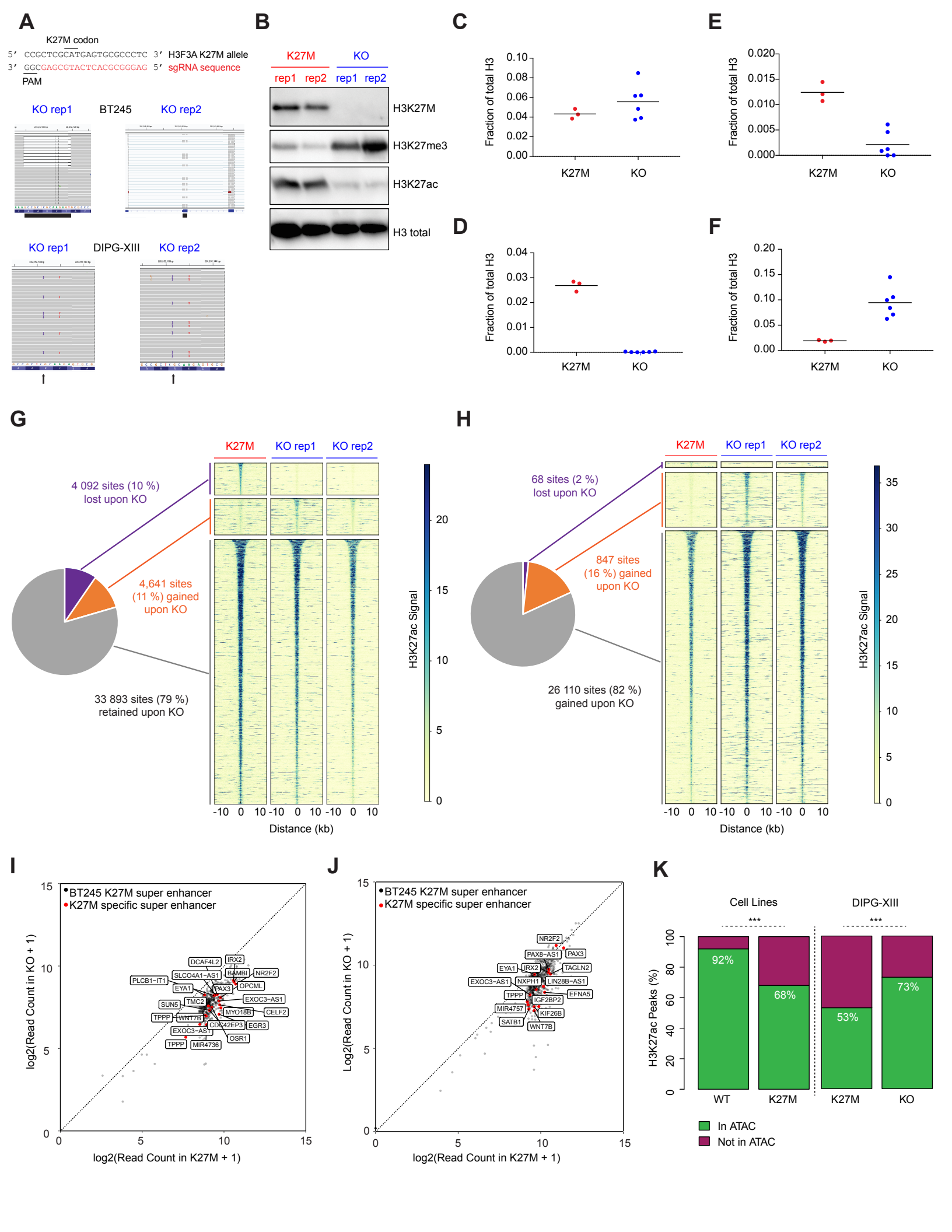
A
K27M codon
5′ CCGCTCGCATGAGTGCGCCCTC 3′ H3F3A K27M allele
3′ GGCGAGCGTACTCACGCGGGAG 5′ sgRNA sequence
PAM
KO rep1
BT245
KO rep2
KO rep1
DIPG-XIII
KO rep2
B
K27M
KO
rep1 rep2 rep1 rep2
H3K27M
H3K27me3
H3K27ac
H3 total
C
Fraction of total H3
K27M
KO
D
Fraction of total H3
K27M
KO
E
Fraction of total H3
K27M
KO
F
Fraction of total H3
K27M
KO
G
K27M
KO rep1
KO rep2
4 092 sites (10 %) lost upon KO
4,641 sites (11 %) gained upon KO
33 893 sites (79 %) retained upon KO
H3K27ac Signal
Distance (kb)
H
K27M
KO rep1
KO rep2
68 sites (2 %) lost upon KO
847 sites (16 %) gained upon KO
26 110 sites (82 %) gained upon KO
H3K27ac Signal
Distance (kb)
I
BT245 K27M super enhancer
K27M specific super enhancer
log2(Read Count in KO + 1)
log2(Read Count in K27M + 1)
DCAF4L2
IRX2
SLCO4A1-AS1
BAMBI
NR2F2
PLCB1-IT1
EYA1
PAX3
OPCML
EXOC3-AS1
SUN5
TMC2
MYO18B
CELF2
TPPP
WNT7B
CDC42EP3
EGR3
EXOC3-AS1
OSR1
TPPP
MIR4736
J
BT245 K27M super enhancer
K27M specific super enhancer
Log2(Read Count in KO + 1)
log2(Read Count in K27M + 1)
NR2F2
PAX8-AS1
PAX3
EYA1
IRX2
TAGLN2
EXOC3-AS1
NXPH1
LIN28B-AS1
TPPP
EFNA5
IGF2BP2
MIR4757
KIF26B
SATB1
WNT7B
K
Cell Lines
DIPG-XIII
***
***
H3K27ac Peaks (%)
92%
68%
53%
73%
WT
K27M
K27M
KO
In ATAC
Not in ATAC

Figure S2. Related to Figure 3.
(A) The sequence of the gRNA used to target the K27M mutant allele of *H3F3A* is shown (top). The tracks of MiSeq data at the target locus demonstrate the insertions and deletions present on the mutant allele, while WT reads are not affected (bottom).
(B-F) Western blot **(B)** and mass spectrometry **(C-F)** of H3WT **(C)** , H3K27M **(D)**, H3K27ac **(E)**, and H3K27me3 **(F)** in BT245 and KO.
(G-H) Pie graphs and heatmaps illustrating number and proportion of gained, lost, and retained H3K27ac sites within DIPG-XIII **(G)** and BT245 **(H)** H3K27M driven models as compared to isogenic KO lines.
(I-J) Dot plot illustrating ChIP-Rx signal (Log2) at H3K27M models BT245 **(I)** and DIPG-XIII **(J)** and the minimal to no observable shift in H3K27ac density upon KO.
(K) ATAC-seq signal demonstrating loss of coherence with H3K27ac peaks between the K27M and WT groups (left) and between the K27M and K27M-KO groups (right). $p<0.001$=***.

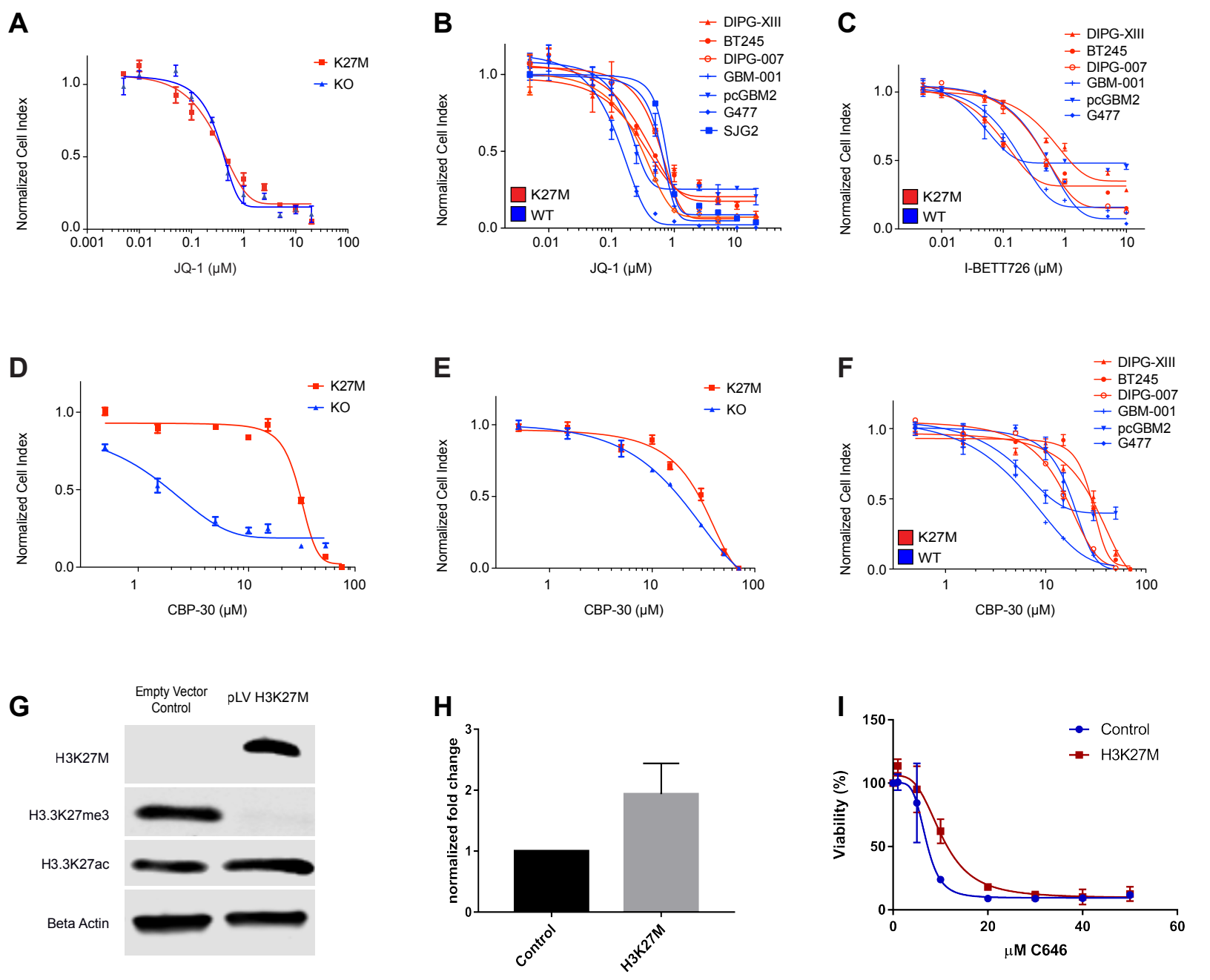
A
Normalized Cell Index
JQ-1 (μM)
K27M
KO
B
DIPG-XIII
BT245
DIPG-007
GBM-001
pcGBM2
G477
SJG2
K27M
WT
C
I-BETT726 (μM)
D
CBP-30 (μM)
E
F
G
Empty Vector Control
pLV H3K27M
H3K27M
H3.3K27me3
H3.3K27ac
Beta Actin
H
normalized fold change
Control
H3K27M
I
Viability (%)
μM C646

Figure S3. Related to Figure 3.
(A) Cell viability of BT245 and isogenic KO lines to bromodomain inhibition by JQ-1.
(B-C) Cell viability of pHGG lines in a 7-day growth assay under treatment with bromodomain inhibitors JQ-1 and I-BET762.
(D-E) Cell viability of BT245 **(D)** and DIPG-XIII **(E)** and corresponding KO control lines to CBP/EP300 inhibitor CBP-30.
(F) Viability of pHGG lines in a 7-day growth assay under treatment with the CBP/EP300 inhibitor CBP-30.
(G) Immunoblot of an immortalized human astrocyte cell line that over-express H3K27M or empty vector control, along with quantification of H3K27me3 and H3K27ac levels.
(H) Quantification of H3K27ac in NSC models that over-express H3K27M as compared to empty vector controls.
(I) Cell viability of astrocytes that over-express H3K27M following treatment with C646 as compared to empty vector controls.

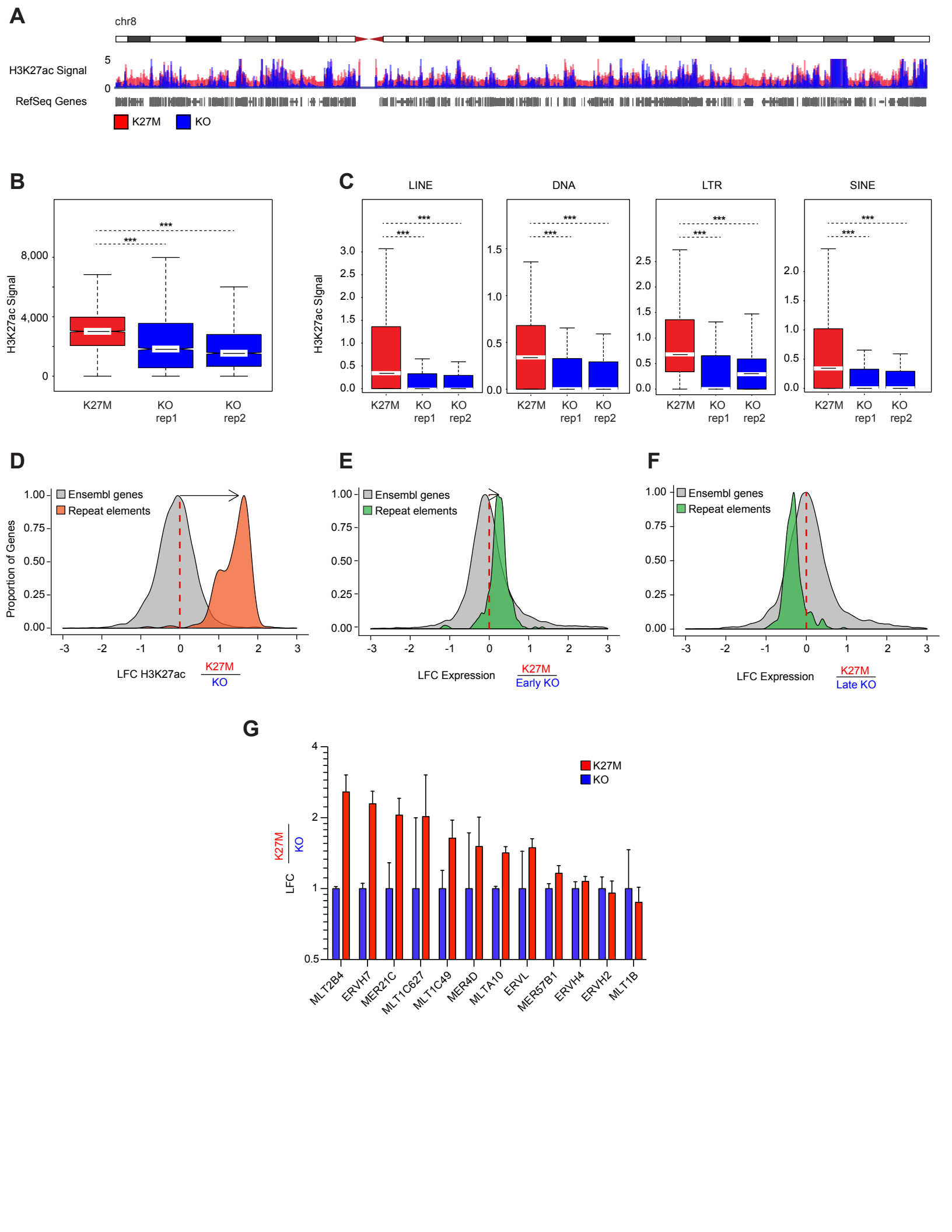
A
chr8
H3K27ac Signal
5
0
RefSeq Genes
K27M
KO
B
H3K27ac Signal
8,000
4,000
0
***
***
K27M
KO rep1
KO rep2
C
LINE
DNA
LTR
SINE
H3K27ac Signal
3.0
2.5
2.0
1.5
1.0
0.5
0.0
1.5
1.0
0.5
0.0
2.5
2.0
1.5
1.0
0.5
0.0
2.0
1.5
1.0
0.5
0.0
***
***
K27M
KO rep1
KO rep2
D
Ensembl genes
Repeat elements
Proportion of Genes
1.00
0.75
0.50
0.25
0.00
-3
-2
-1
0
1
2
3
LFC H3K27ac
K27M
KO
E
Ensembl genes
Repeat elements
LFC Expression
K27M
Early KO
F
Ensembl genes
Repeat elements
LFC Expression
K27M
Late KO
G
K27M
KO
LFC
4
2
1
0.5
MLT2B4
ERVH7
MER21C
MLT1C627
MLT1C49
MER4D
MLTA10
ERVL
MER57B1
ERVH4
ERVH2
MLT1B

Figure S4. Related to Figure 4.
(A) Quantitative ChIP-Rx scaled reads between BT245 K27M (red) and KO (blue) cell cultures across chromosome 8.
(B) Enrichment of H3K27ac across the human genome in one megabase windows comparing BT245 versus KO clones using a Wilcoxon rank sum test. $p<0.001$=***. The horizontal line inside the box corresponds to the median, the lines above and below the box delimit the interquartile range (IQR), and the end of the whiskers delimit values up to 1.5 times the IQR.
(C) Enrichment of H3K27ac across repetitive regions (LINE, DNA, LTR, SINE) of the human genome annotated by the RepeatMasker database comparing BT245 vs KO using a Wilcoxon rank sum test. $p<0.001$=***.
(D-F) Changes in deposition of H3K27ac over repetitive elements in BT245 (n=2) relative to KO (n=1) **(D)** and in expression of repetitive elements in in BT245 (n=5) relative to early-passage KO lines that represent the effect of K27M-KO (n=3) **(E)** and late-passage KO that may have lost the effect of H3K27me3 restoration through passaging (n=2) **(F)**. Histograms showing the distributions of the log2 fold-change (LFC) of genomic features in K27M relative to KO. Orange: H3K27ac deposition over repetitive elements (Repbase). Green: transcription of repetitive elements (Repbase). Grey: H3K27ac (left) and transcription (middle and right) of Ensembl genes (GRCh37). Elements with sufficiently high expression (baseMean > 100) and LFCs in [-3,3] range shown here.
(G) Measurement of expression of a panel of ERV families by droplet digital PCR (ddPCR) in H3K27M lines compared to respective KO lines. Plots show mean +SEM of 3 experimental replicates, BT245 cell line. Y-axis is in log2 scale.

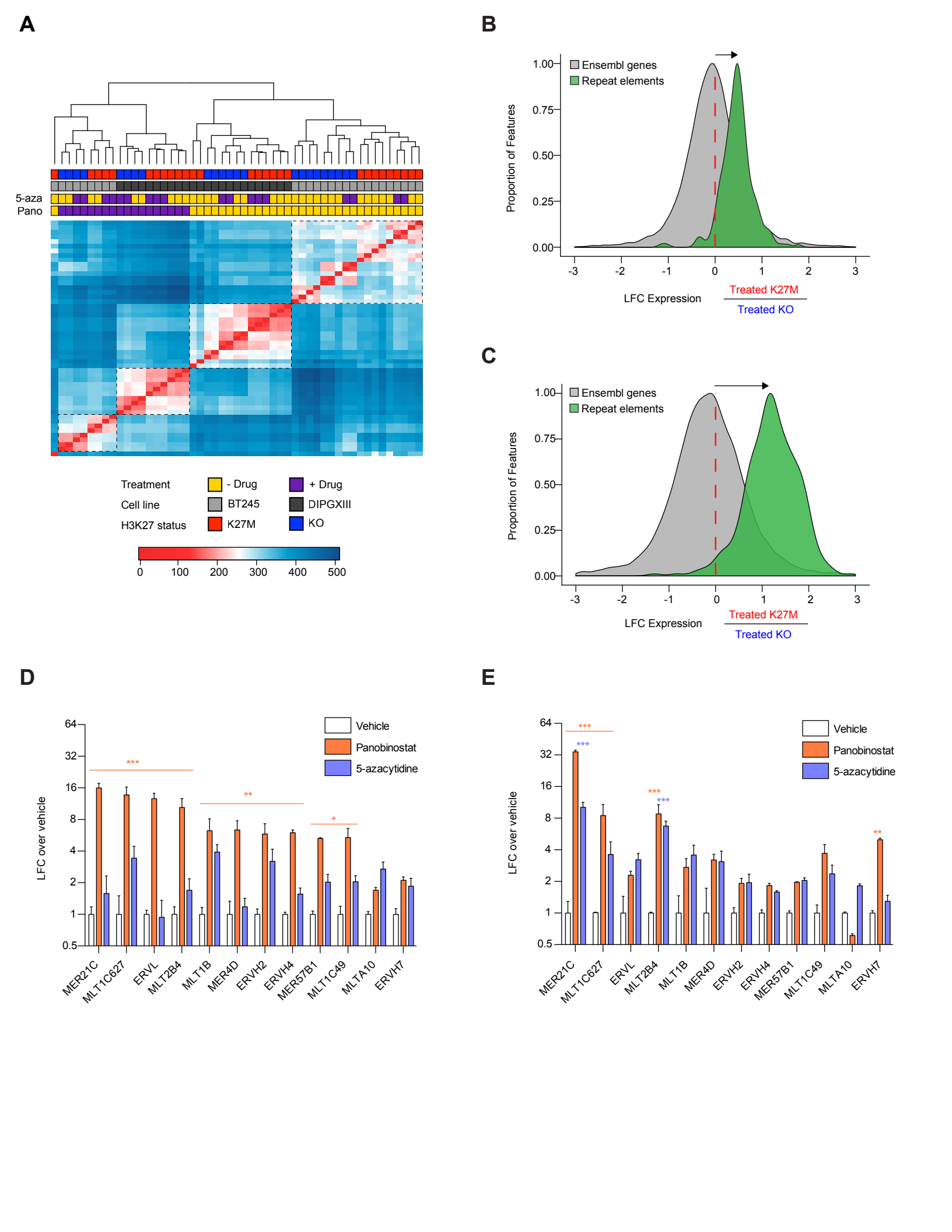
A
5-aza
Pano
Treatment
- Drug
+ Drug
Cell line
BT245
DIPGXIII
H3K27 status
K27M
KO
0
100
200
300
400
500
B
Ensembl genes
Repeat elements
Proportion of Features
1.00
0.75
0.50
0.25
0.00
-3
-2
-1
0
1
2
3
LFC Expression
Treated K27M
Treated KO
C
Ensembl genes
Repeat elements
Proportion of Features
LFC Expression
Treated K27M
Treated KO
D
Vehicle
Panobinostat
5-azacytidine
LFC over vehicle
64
32
16
8
4
2
1
0.5
***
**
*
MER21C
MLT1C627
ERVL
MLT2B4
MLT1B
MER4D
ERVH2
ERVH4
MER57B1
MLT1C49
MLTA10
ERVH7
E
Vehicle
Panobinostat
5-azacytidine
LFC over vehicle
***
***
***
***
**
MER21C
MLT1C627
ERVL
MLT2B4
MLT1B
MER4D
ERVH2
ERVH4
MER57B1
MLT1C49
MLTA10
ERVH7

Figure S5. Related to Figure 6.
(A) Hierarchical clustering of samples based on global transcriptomic profiles. Color key: low (blue) to high (red) similarity between pairs of samples. Similarity between samples is calculated using the Euclidean distance over their variant-stabilizing-transformed transcriptomic profiles.
(B-C) Changes in expression of repetitive elements in K27M relative to KO after combination treatment (panobinostat and 5-azacytidine) for both DIPG-XIII (n=3) relative to KO (n=2) **(B)** and BT245 (n=2) relative to KO (n=2) **(C)**. Histograms showing the distributions of the log2 fold-change (LFC) of transcription of repetitive elements (green; Repbase) and Ensembl genes (grey; GRCh37) in K27M relative to KO. Elements with sufficiently high expression (baseMean > 100) and LFCs in [-3,3] range shown here.
(D-E) Measurement of ERV family expression by ddPCR upon 48 hour treatment with panobinostat (50 nM) or 5-azacytdine 5 μM), normalized to vehicle control in BT245 **(D)** and corresponding KO lines **(E)**. Plots show mean +SEM of 3 experimental replicates of the BT245 line. Two-way analysis of variance compares vehicle to each drug, with Bonferroni posttest significance shown by $p<0.001$=***, $p<0.01$=**, $p<0.05$=*. Y-axis is in log2 scale.

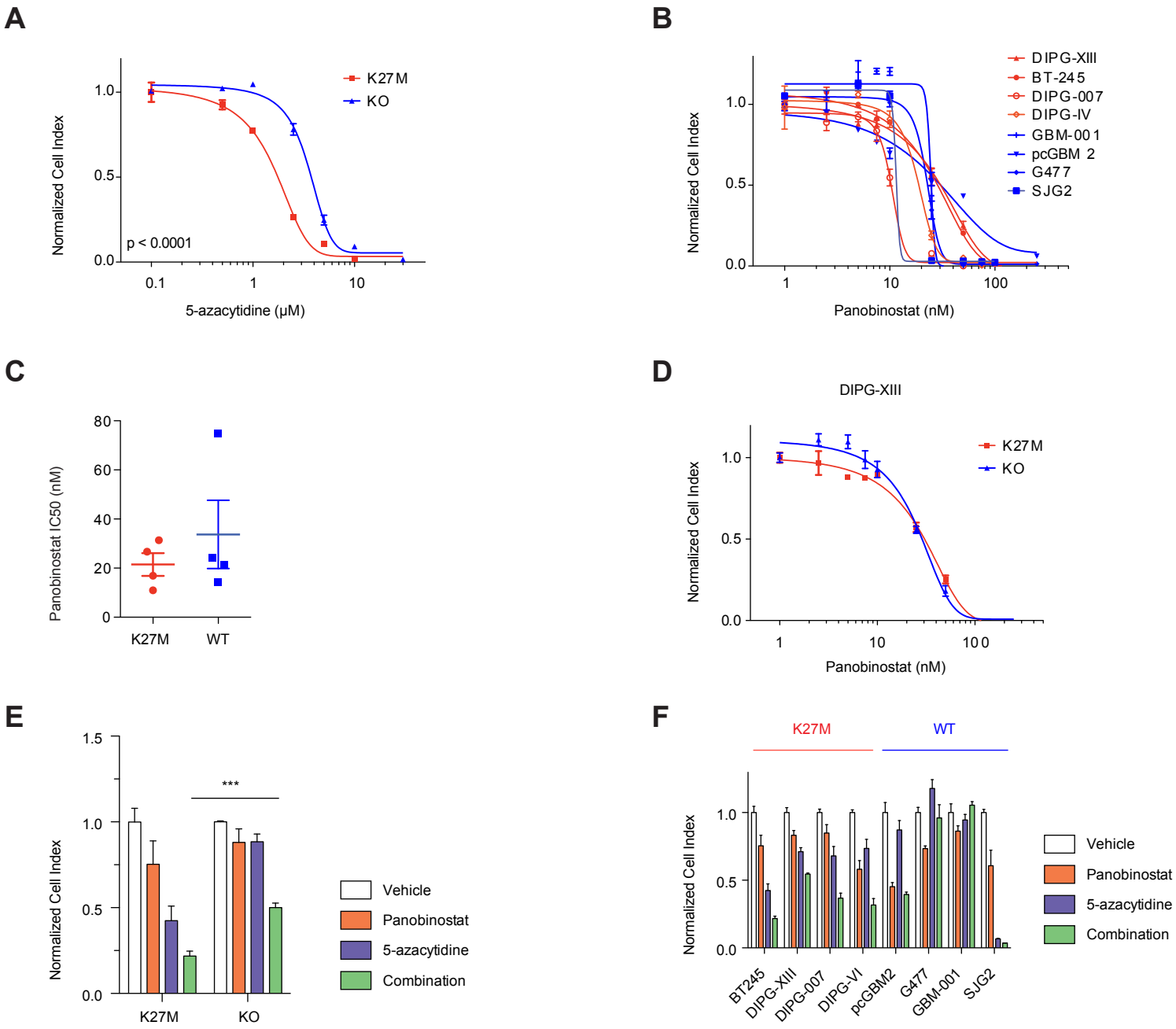
A
Normalized Cell Index
1.0
0.5
0.0
K27M
KO
p < 0.0001
0.1
1
10
5-azacytidine (μM)
B
Normalized Cell Index
1.0
0.5
0.0
DIPG-XIII
BT-245
DIPG-007
DIPG-IV
GBM-001
pcGBM 2
G477
SJG2
1
10
100
Panobinostat (nM)
C
Panobinostat IC50 (nM)
80
60
40
20
0
K27M
WT
D
DIPG-XIII
Normalized Cell Index
1.0
0.5
0.0
K27M
KO
1
10
100
Panobinostat (nM)
E
Normalized Cell Index
1.5
1.0
0.5
0.0
***
K27M
KO
Vehicle
Panobinostat
5-azacytidine
Combination
F
K27M
WT
Normalized Cell Index
1.0
0.5
0.0
BT245
DIPG-XIII
DIPG-007
DIPG-VI
pcGBM2
G477
GBM-001
SJG2
Vehicle
Panobinostat
5-azacytidine
Combination

Figure S6. Related to Figure 6.
(A) Dose response curves of H3K27M and KO lines of BT245 to 5-azacytidine in isogenic context. Plots show mean +/-SEM of 3 experimental replicates.
(B-C) Cell viability of H3.3K27M and WT cells in a 7-day growth assay across a panel of pHGG lines **(B)** and corresponding IC50 values **(C)**.
(D) Dose response curves of H3K27M and KO lines of DIPG-XIII to 5-azacytidine in isogenic context. Plots show mean +/-SEM of 3 experimental replicates.
(E-F) Cell viability in 7-day growth assay under treatment of lines with sub-IC50 doses of panobinostat (15 nM), 5-azacytidine (1.5 μM) and their combination in BT245 versus KO **(E)** and to H3.3K27M compared to WT cell lines **(F)**. Plots show mean +SEM of 3 experimental replicates. A two-tailed t-test compares combination treated lines, with $p<0.001$=***.

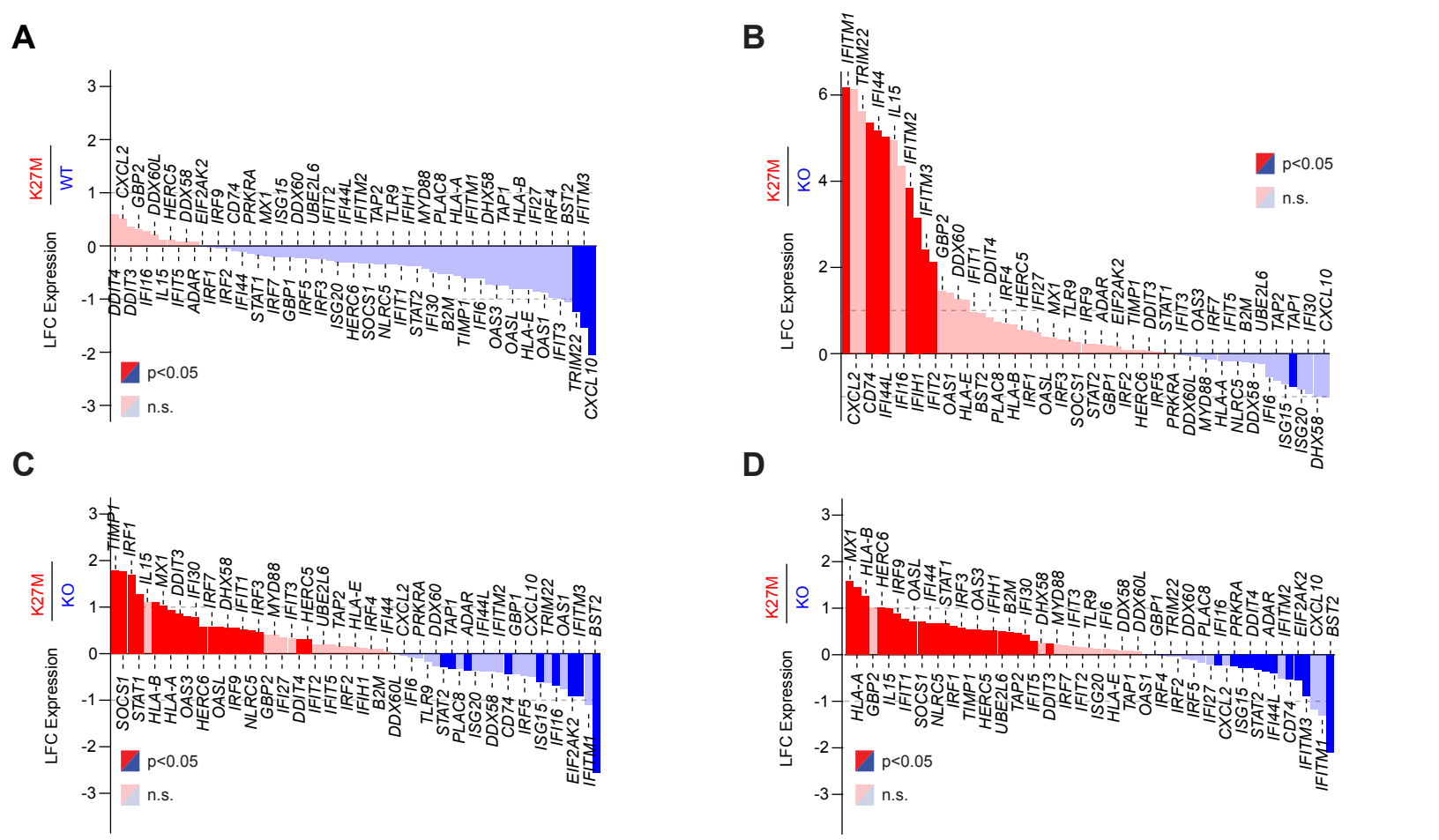

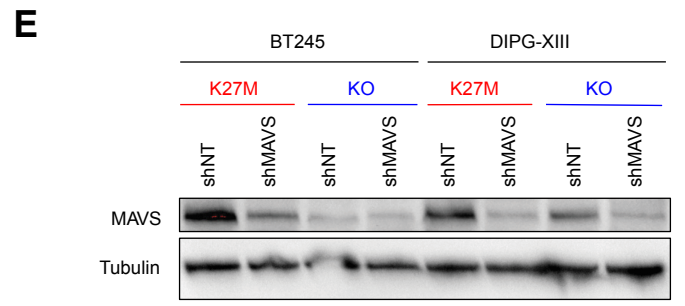

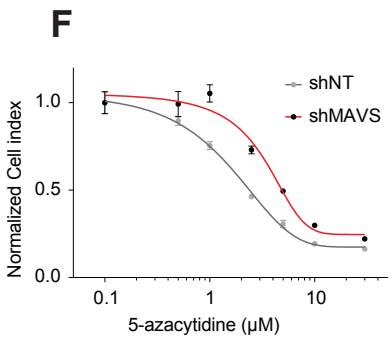

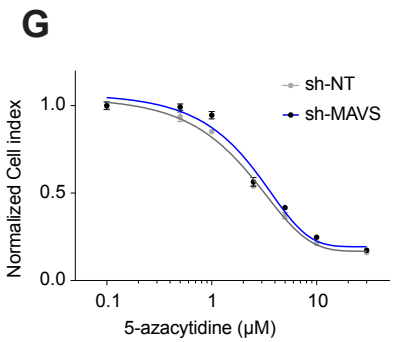

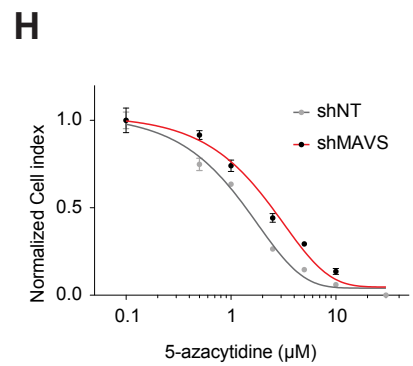

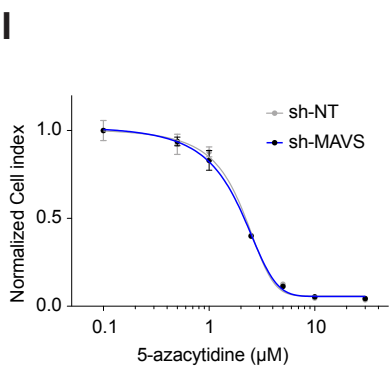

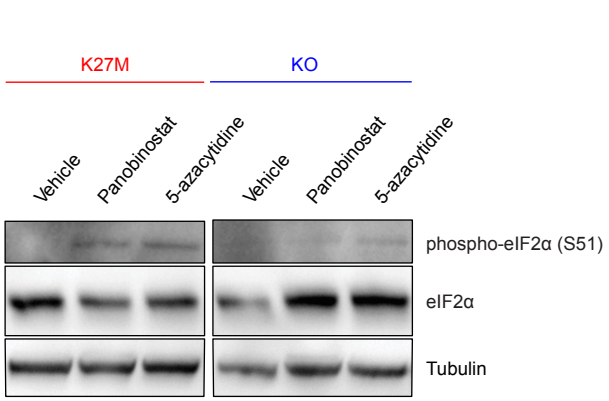

K

DIPG XIII				
	DMSO	Panobinostat	5-aza	combo
Median survival	86	95	107	125
BT245				
	DMSO	Panobinostat	5-aza	combo
Median survival	110	131	143	155
pcGBM2				
	DMSO	Panobinostat	5-aza	combo
Median survival	85	101	90	96

Figure S7. Related to Figure 7.

(A-B) Waterfall plot illustrating changes in the expression levels of the interferon response genes in H3.3K27M HGG tumors (n=17) compared to H3K27WT (n=15) **(A)** and in BT245 cell line (n=5) relative to KO (n=5) at baseline **(B)**. Y-axis: log2 fold-change of expression in K27M relative to K27WT or KO. Red: upregulated genes in K27M. Blue: downregulated genes. Significantly deregulated genes highlighted ($p \leq 0.05$; baseMean$\geq$100).

(C-D) Waterfall plots illustrating the induction of interferon response genes in DIPG-XIII relative to KO upon treatment with panobinostat and 5-azacytidine **(C)** and panobinostat alone **(D)**. Y-axis: log2 fold-change of expression in K27M relative to KO (combination DIPG-XIII n=3, DIPG-XIII-KO n=2; panobinostat DIPG-XIII n=3, DIPG-XIII n=2).

(E) Western blot demonstrates decreased expression of MAVS protein (57 kD band) by shRNA targeting.

(F-I) Dose response curves to 5-azacytidine in a 7-day growth assay of H3.3K27M and KO lines of DIPG-XIII **(F-G)** and BT245 **(H-I)** transduced with lentiviral vectors expressing short hairpin RNA (shRNA) controls (non-targeting, NT) or a pool of 4 shRNAs targeting MAVS. Plots show mean +/-SEM of 3 experimental replicates.

(J) Western blot of phosphorylated eIF2-alpha upon 48 hours treatment with panobinostat (50 nM) or 5-azacytidine (5 μM) in BT245 and KO lines.

(K) Summary of median survivals of mice bearing PDX models of DIPGXIII, BT245, and pcGBM2 following treatment with DMSO, panobinostat, 5-azacytidine, and combination as related to **Figures 7E-F**.